

Structural Optimization Simulation of MHPA-PV/T Module for Xizang

Li Wan

Tibet Autonomous Region Energy Research Demonstration Center, Lasa Tibet, 850000, China

xizangnengyuan@163.com

Abstract

This article establishes a mathematical model for the operation of MHPA-PVT system and uses Fluent simulation software to build a three-dimensional steady-state model of MHPA-PVT components. Based on the verification of the reliability of the model, optimization research is conducted on the laying, arrangement direction, and condensation section length of the micro heat pipe array. Taking into account the cost, benefits during use, and service life, the component is still the most suitable for a fully deployed micro heat pipe array; The arrangement directions of different micro heat pipe arrays (horizontal and vertical) have little difference in the thermal and electrical performance of the components; The increase in the length of the condensation section can improve the power generation efficiency, but it will reduce the heat collection efficiency.

Keywords

Xizang; MHPA-PV/T Components; Structural Optimization; Simulation Study.

1. Introduction

With the continuous advancement of industrialization in China and the sharp increase in energy consumption, China has become the world's largest consumer of coal and the second largest consumer of oil and electricity. In the short term, the sharp increase in energy consumption has led to "electricity shortage", "oil shortage" and "coal shortage" in many parts of China, while non renewable resources such as fossil fuels and water resources are becoming increasingly scarce [1]. From the perspective of energy conservation, there are two ways to explore energy: open source and throttling. Open source refers to finding various renewable energy sources that can replace existing energy sources, while throttling refers to exploring more energy utilization methods on the basis of existing energy sources, achieving cascading energy utilization, and obtaining maximum energy utilization efficiency [2].

Sandnes from the University of Oslo in Norway [3] developed a flat box PV/T collector made of PPO plastic. Experimental studies were conducted on the collector (T), PV/T collector without glass cover plate (PV/T), and PV/T collector with glass cover plate (PV/Tg) at lower water temperatures, and the photothermal performance of different systems was simulated. Hisashi et al. [4] from Hokkaido University in Japan tested a tube plate PV/T system with a glass cover plate at a constant inlet temperature. The system's electrical efficiency was 10-13% and thermal efficiency was 40-50%, lower than the thermal efficiency of an independent solar water heating system. Although the overall efficiency of the PV/T system is roughly equal to that of an independent solar water heating system, the system's available energy efficiency is much higher than that of independent solar water heating systems and photovoltaic systems. Gang P [5] constructed a PV/T collector based on circular heat pipes, and experimental and simulation results showed that the daily average thermal efficiency and electrical efficiency of the collector were 41.9% and 9.4%, respectively. Meysam Moradgholi et al. [6] designed a heat pipe solar

photovoltaic thermal PV/T system, which uses a heat pipe to absorb the heat of photovoltaic cells at an isothermal temperature, and tested it in spring and summer. In spring, when the inclination angle of the photovoltaic panel is 30 ° and the working medium of the heat pipe is methanol, the system outputs an average of 5.67% more electricity than a standalone photovoltaic system, and the thermal efficiency is 16.35%; In summer, when the inclination angle of the photovoltaic panel is 40 ° and the heat pipe medium is acetone, the system outputs an average of 7.7% more electricity than a standalone photovoltaic system, while the thermal efficiency is 45.14%.

This article establishes a mathematical model for the operation of MHPA-PVT system and uses Fluent simulation software to build a three-dimensional steady-state model of MHPA-PVT components. On the basis of ensuring the reliability of the model, optimization research is conducted on the laying, layout direction, and condensation section length of the micro heat pipe array, providing theoretical basis for the optimization of the structure and performance of the components.

2. Mathematical Model

The conservation of mass equation, also known as the continuity equation, is mathematically expressed as [7]:

$$\frac{\partial \rho}{\partial t} + \frac{\partial(\rho u)}{\partial x} + \frac{\partial(\rho v)}{\partial y} + \frac{\partial(\rho w)}{\partial z} = 0 \quad (1)$$

Momentum conservation equation:

For incompressible fluids with constant viscosity, the momentum conservation equations in the i , j , and k directions are expressed as:

The momentum equation of i :

$$\frac{\partial (u_i)}{\partial t} + \text{div}(u_i U) = -\frac{\partial p}{\partial x_i} + \text{div}(\eta \text{grad} u_i) \quad (2)$$

The momentum equation of j :

$$\frac{\partial (u_j)}{\partial t} + \text{div}(u_j U) = -\frac{\partial p}{\partial x_j} + \text{div}(\eta \text{grad} u_j) \quad (3)$$

The momentum equation of k :

$$\frac{\partial (u_k)}{\partial t} + \text{div}(u_k U) = -\frac{\partial p}{\partial x_k} + \text{div}(\eta \text{grad} u_k) \quad (4)$$

Energy conservation equation:

The law of conservation of energy is actually the first law of thermodynamics. The expression is as follows:

$$\frac{\partial(\rho T)}{\partial t} + \frac{\partial(\rho u T)}{\partial x} + \frac{\partial(\rho v T)}{\partial y} + \frac{\partial(\rho w T)}{\partial z} = \frac{\partial}{\partial x} \left(\frac{k}{c_p} \cdot \frac{\partial T}{\partial x} \right) + \frac{\partial}{\partial y} \left(\frac{k}{c_p} \cdot \frac{\partial T}{\partial y} \right) + \frac{\partial}{\partial z} \left(\frac{k}{c_p} \cdot \frac{\partial T}{\partial z} \right) + S_T \quad (5)$$

Basic equation of turbulence:

The application of the standard k - ε two equation model is currently the main method for engineering flow and heat transfer problems, and this model is also used for numerical simulation in this paper [8]. Turbulent pulsation kinetic energy equation, also known as k equation:

$$\rho \frac{\partial k}{\partial t} + \rho u_j \frac{\partial k}{\partial x_j} = \frac{\partial}{\partial x_j} \left(\eta + \frac{\eta_t}{\sigma_k} \right) + \eta_t \frac{\partial u_i}{\partial x_j} \left(\frac{\partial u_j}{\partial x_i} + \frac{\partial u_i}{\partial x_j} \right) - \rho \varepsilon \quad (6)$$

The governing equation for dissipation rate ε :

$$\rho \frac{\partial \varepsilon}{\partial t} + \rho u_k \frac{\partial \varepsilon}{\partial x_k} = \frac{\partial}{\partial x_k} \left(\eta + \frac{\eta_t}{\sigma_k} \right) + \frac{c_1 \varepsilon}{k} \eta_t \frac{\partial u_i}{\partial x_j} \left(\frac{\partial u_j}{\partial x_i} + \frac{\partial u_i}{\partial x_j} \right) - c_2 \rho \frac{\varepsilon^2}{k} \quad (7)$$

When using the k - ε model, the equation for the turbulent viscosity coefficient η_t is expressed as follows [9]:

$$\eta_t = \frac{c_\mu \rho k^2}{\varepsilon} \quad (8)$$

3. The Impact of Laying Micro Heat Pipe Arrays on Performance

Due to the flat shape of the micro heat pipe array, it can be easily attached to the TPT back plate of photovoltaic cells. Currently, MHPA-PVT modules are almost fully covered with micro heat pipe arrays. However, considering cost issues, we are exploring whether reducing the number of micro heat pipe arrays can achieve near full coverage of power generation and heat collection effects. For this purpose, Fluent models were established for fully laying, laying 20 and 17 micro heat pipe arrays (with dimensions of $808 \times 60 \times 3\text{mm}$), as shown in Figures 1 and 2.

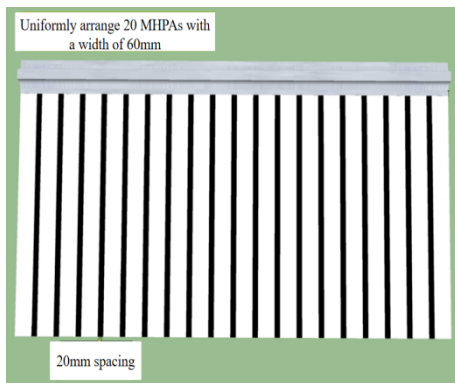


Fig 1. The schematic of component's back bonding 20 MHPA

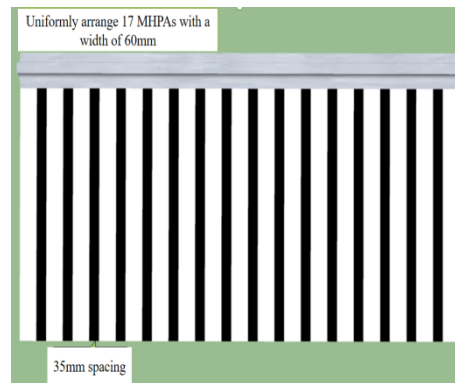


Fig 2. The schematic of component's back bonding 17 MHPA

The calculation results are summarized in Figures 3 to 6. The simulation results show that compared with a fully laid micro heat pipe array, the thermal efficiency, electrical efficiency, and overall efficiency of laying 20 and 17 heat pipes all decrease, and the less heat pipes laid, the greater the decrease in efficiency. From the perspective of thermal efficiency, the decrease in thermal efficiency is more significant when compared to the full laying of 20, but the decrease in thermal efficiency is smaller when compared to the laying of 17. For example, when the inlet temperature is 10°C , the thermal efficiency of full laying, laying of 20, and laying of 17 is 51.3%, 44.5%, or 44.0%, respectively. From the perspective of electrical efficiency, under the same inlet temperature conditions, the electrical efficiency decreases by about 0.2% each time from full laying to laying 20, and then to laying 17. The variation law of electrical efficiency can also be seen on the curve of the average temperature of the battery, as shown in Figure 6. Reducing the laying of heat pipes not only causes an increase in battery temperature, but also increases the unevenness of battery temperature distribution.

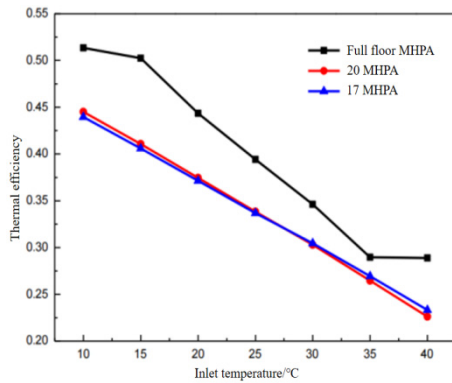


Fig 3. The change curve of thermal efficiency under different MHPA laying with inlet Temperature

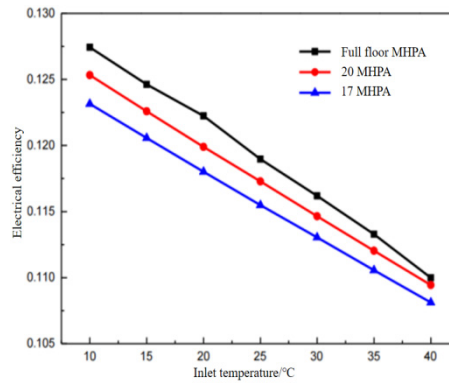


Fig 4. The change curve of power generation efficiency under different MHPA laying with inlet temperature

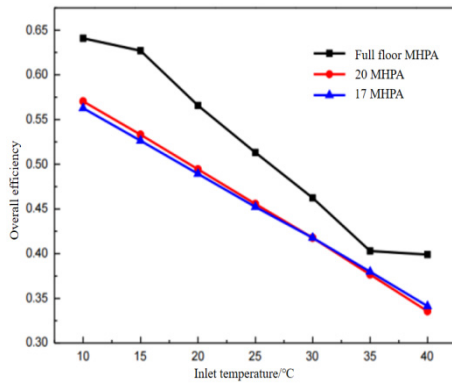


Fig 5. The change curve of total efficiency under different MHPA laying with inlet temperature

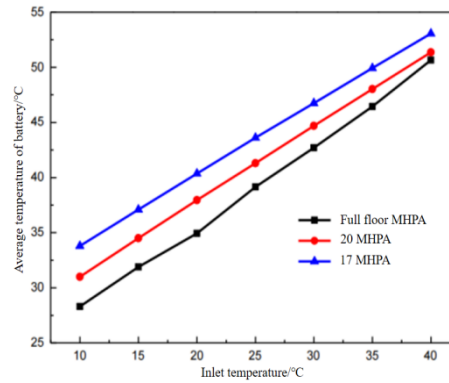


Fig 6. The change curve of PV's temperature under different MHPA laying with inlet temperature

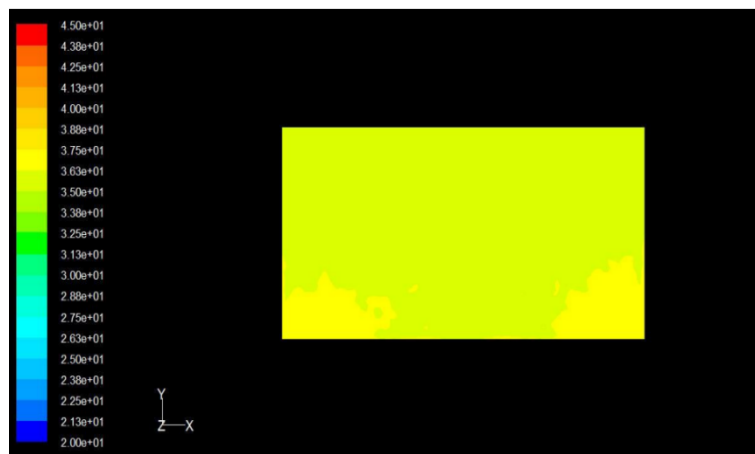


Fig 7. $t_i=20^\circ\text{C}$, Temperature contours when the battery level paved MHPA

Due to the fact that the temperature of the battery backplate without the attached micro heat pipe array is higher than that of the attached part under non full coverage conditions, the heat in this area can only be transferred to the attached micro heat pipe array through thermal conduction. However, in terms of speed, the difference is too large compared to the high-efficiency heat transfer element micro heat pipe array, resulting in a certain degree of heat accumulation in this area. This can be intuitively seen on the temperature distribution cloud map of the battery layer at an inlet temperature of 20 °C in the three Fluent software simulation

scenarios, as shown in Figures 7 to 9. The uneven temperature of the battery not only affects the power generation and heat collection efficiency of the components, but also seriously affects the service life of the components. Therefore, considering the cost, benefits during use, and service life, the components are still the most suitable for fully laid micro heat pipe arrays.

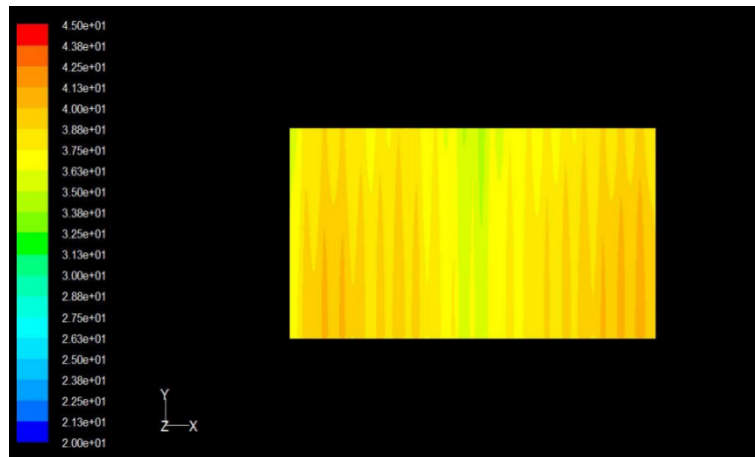


Fig 8. $t_i=20^{\circ}\text{C}$, Temperature contours when the battery level bonding 20 MHPA

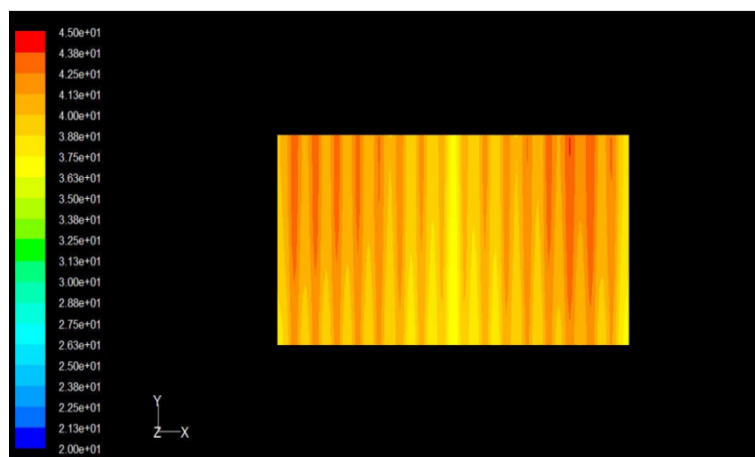


Fig 9. $t_i=20^{\circ}\text{C}$, Temperature contours when the battery level bonding 17 MHPA

4. The Impact of Layout Direction on Performance



Fig 10. The physical pictures of horizontal and vertical components

In addition to the arrangement of heat pipes, the distribution of length between the evaporation and condensation sections of the heat pipe also has a significant impact on the efficiency of the component's power generation and heat collection. Here, we first compare the performance of a 1580×808mm component under horizontal (i.e. heat pipe length of 808mm) and vertical (i.e. heat pipe length of 1580mm) conditions. Secondly, under horizontal conditions, the width of

the wing shaped water tube heat exchanger (i.e. condensation section length) is set to 80, 100, and 120mm, respectively, to compare their performance.

Under the conditions of optimized flow rate of $0.15\text{kg}/(\text{m}^2\cdot\text{s})$, total solar irradiance $G=800\text{W}/\text{m}^2$, ambient temperature $t_a=20^\circ\text{C}$, and instantaneous wind speed $u=0.5\text{m}/\text{s}$, models of horizontal and vertical components were established and calculated in *Fluent software*. The results are summarized in Figures 11 to 14. It can be found that at lower inlet temperatures (t_i is 10°C and 15°C), the thermal and electrical efficiencies of horizontal and vertical components are comparable, and the battery temperature is also very close; As the inlet temperature increases, the average temperature of the vertical component battery is about $1.5\text{-}2.0^\circ\text{C}$ higher than that of the horizontal component, with a thermal efficiency $3\text{-}5\%$ higher and an electrical efficiency about 0.2% lower. Therefore, in this environment, horizontal components have a good cooling effect on the battery, but vertical components have a better heat collection effect.

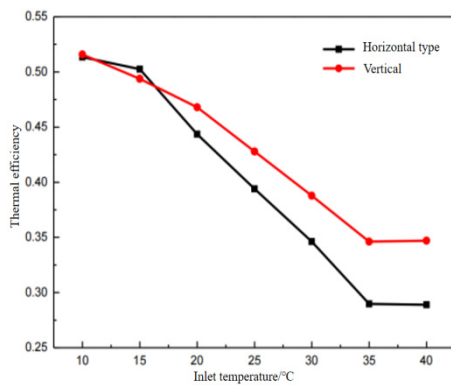


Fig 11. When $t_a=20^\circ\text{C}$, $u=0.5\text{m}/\text{s}$, the thermal efficiency of horizontal and vertical components under different inlet temperature

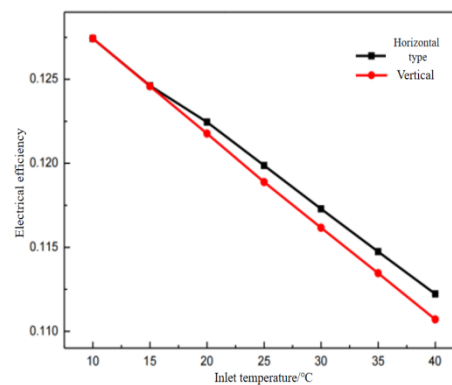


Fig 12. When $t_a=20^\circ\text{C}$, $u=0.5\text{m}/\text{s}$, the power generation efficiency of horizontal and vertical components under different inlet temperature

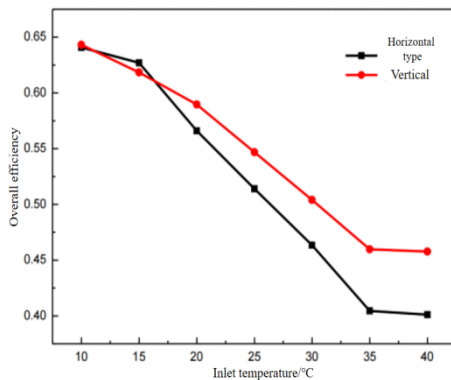


Fig 13. When $t_a=20^\circ\text{C}$, $u=0.5\text{m}/\text{s}$, the total efficiency of horizontal and vertical components under different inlet temperature

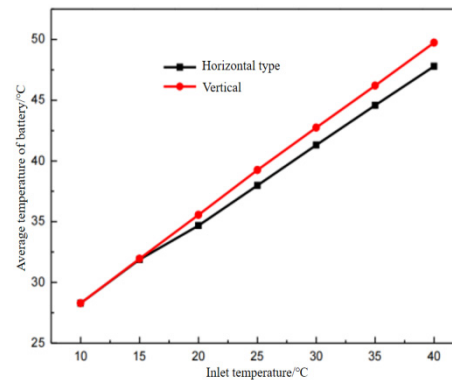


Fig 14. When $t_a=20^\circ\text{C}$, $u=0.5\text{m}/\text{s}$, the PV's temperature of horizontal and vertical components under different inlet temperature

In order to further compare the performance of horizontal and vertical components under other environmental conditions, this paper changed the environmental temperature t_a to 10°C , the instantaneous wind speed u to $2\text{m}/\text{s}$, the flow rate to continue at $0.15\text{kg}/(\text{m}^2\cdot\text{s})$, and the total solar irradiance G to continue at $800\text{W}/\text{m}^2$. The calculated results of the performance of horizontal and vertical components are shown in Figures 15 to 17. It can be seen that under

this condition, there is almost no difference in the performance of horizontal and vertical components.

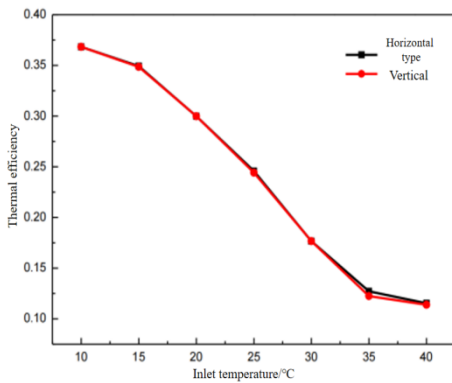


Fig 15. When $t_a=10^\circ\text{C}$, $u=2\text{m/s}$, the thermal efficiency of horizontal and vertical components under different inlet temperature

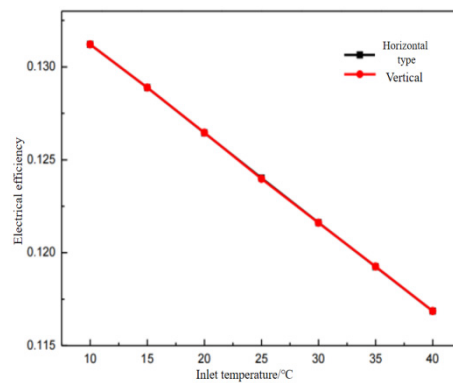


Fig 16. When $t_a=10^\circ\text{C}$, $u=2\text{m/s}$, the power generation efficiency of horizontal and vertical components under different inlet temperature

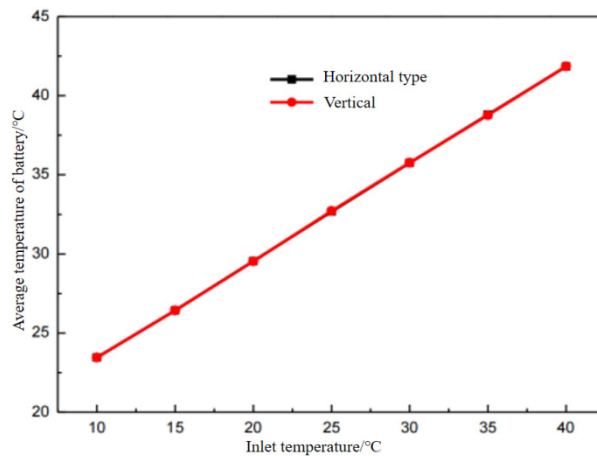


Fig 17. When $t_a=10^\circ\text{C}$, $u=2\text{m/s}$, the PV's temperature of horizontal and vertical components under different inlet temperature

5. The Impact of Condensation Section Length on Performance

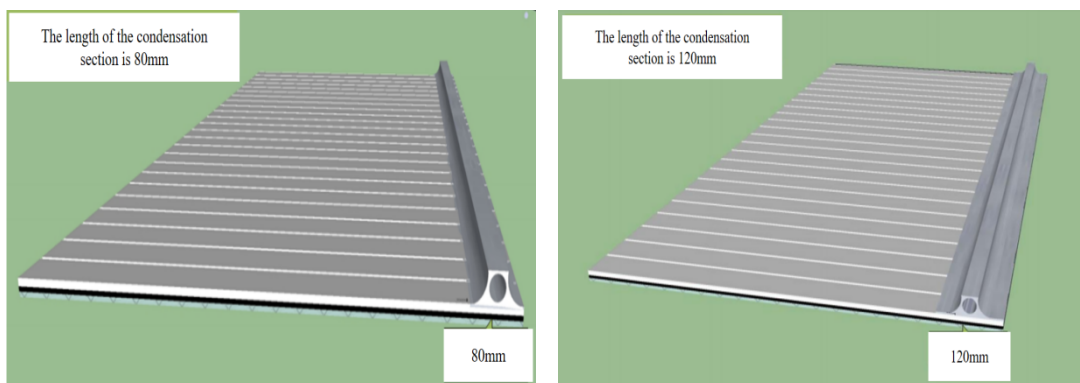


Fig 18. Simulation diagram of a component with a condensation section length of 80mm and 120mm

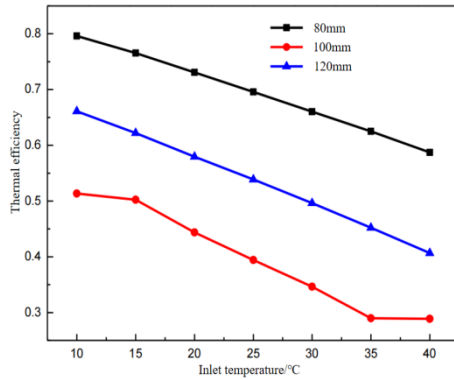


Fig 19. When $t_a=20^\circ\text{C}$, $u=0.5\text{m/s}$, the thermal efficiency of different condensation zone length's components under different inlet temperature

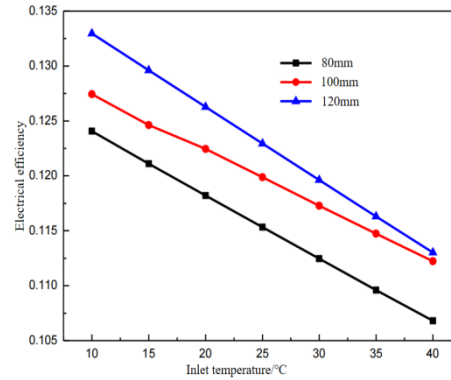


Fig 20. When $t_a=20^\circ\text{C}$, $u=0.5\text{m/s}$, the power generation efficiency of different condensation zone length's components under different inlet temperature

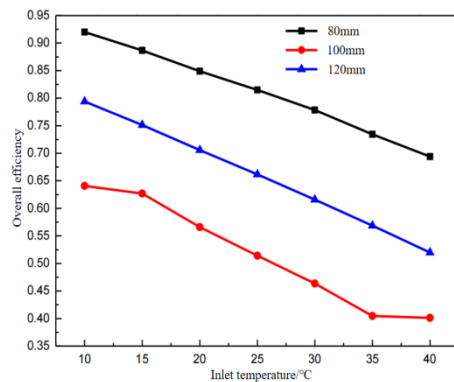


Fig 21. When $t_a=20^\circ\text{C}$, $u=0.5\text{m/s}$, the total efficiency of different condensation zone length's components under different inlet temperature

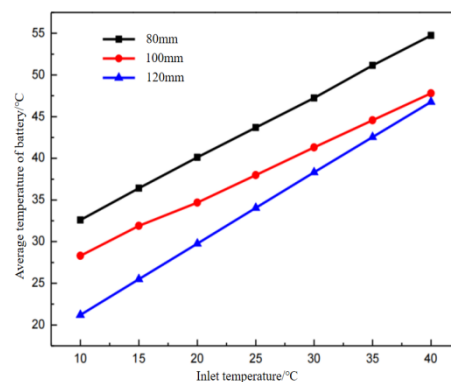


Fig 22. When $t_a=20^\circ\text{C}$, $u=0.5\text{m/s}$, the PV's temperature of different condensation zone length's components under different inlet temperature

Considering that the installation and use of horizontal components are relatively convenient in practical applications, we will continue to optimize the width of the wing shaped water tube heat exchanger with horizontal components. MHPA-PV/T component models of wing shaped water tube heat exchangers with widths of 80 and 120mm were established, and simulation diagrams are shown in Figures 18. Combined with existing components (condensing section length of 100mm), the calculation results are summarized in Figures 19 to 22.

In Figure 22, it can be clearly seen that as the length of the condensation section increases, the temperature of the battery decreases significantly. When the inlet temperature of the component is 20°C and the length of the condensation section is 120mm, the temperature of the battery is 29.8°C , which is 4.9°C and 10.3°C lower than the condensation sections of 100mm and 80mm, respectively. The power generation efficiency is directly related to the battery temperature. When the length of the condensation section is 120mm, the power generation efficiency is 12.6%, which is 0.4% and 0.8% higher than the condensation sections of 100mm and 80mm, respectively. When the length of the condensation section is 80mm, although the high temperature of the battery causes a decrease in power generation efficiency, the heat collection efficiency is higher than other condensation section lengths due to the large temperature difference between the battery and water. Overall, increasing the length of the

condensation section can improve power generation efficiency, but it will reduce heat collection efficiency. The specific optimization length still needs to be further studied by establishing a model.

6. Conclusion

(a) Compared with a fully laid micro heat pipe array, laying 20 and 17 heat pipes resulted in a decrease in thermal efficiency, electrical efficiency, and overall efficiency. The fewer heat pipes laid, the greater the decrease in efficiency. Taking into account cost, benefits during use, and service life, the component is still the most suitable for a fully laid micro heat pipe array.

(b) The arrangement of different micro heat pipe arrays (horizontal and vertical) results in little difference in the thermal and electrical performance of the components.

(c) As the length of the condensation section increases, the temperature of the battery decreases significantly. Overall, increasing the length of the condensation section can improve power generation efficiency, but it will reduce heat collection efficiency. The specific optimization length still needs to be further studied by establishing a model.

Acknowledgments

“Experimental Study on the Performance of MHPA-PV/T Heat Pump System Suitable for High Altitude” (XZ202501ZR0067).

References

- [1] Development of Solar Thermal Utilization Industry: Review and Prospect Building technology 2011, (24): 22-25.
- [2] Dai Tianhong, Zhang Zhu Calculation of the product of effective transmittance and absorption of flat panel solar air collectors Journal of Solar Energy 1996, (04):303-307.
- [3] B. Sandnes and J. Rekstad. A Photovoltaic/Thermal (PV/T) Collector with a Polymer Absorber Plate. Solar Energy. 2015, 72(1): 63-73.
- [4] H. Saitoh, Y. Hamada, H. Kubota and E. Al. Field Experiments and Analyses On a Hybrid Solar Collector. Applied Thermal Engineering. 2018, 23(16): 2089-2105.
- [5] Gang P, Huide F, Tao Z, et al. A numerical and experimental study on a heat pipe PV/T system [J]. Solar Energy, 2017, 85(5): 911-921.
- [6] Meysam Moradgholi, Seyed Mostafa Nowee, Iman Abrishamchi. Application of heat pipe in an experimental investigation on a novel photovoltaic/thermal(PV/T) system [J]. Solar Energy. 2014 (107): 82-88.
- [7] Wang Fujun Computational Fluid Dynamics Analysis: Principles and Applications of CFD Software Tsinghua University Press Co., Ltd., 2004.
- [8] Zhang Zixiong, Dong Zengnan Viscous fluid mechanics Tsinghua University Press Co., Ltd., 1998.
- [9] Fu Dexun, Ma Yanwen Computational fluid dynamics Higher Education Press, 2002.